HETEROCYCLES, Vol. 102, No. 9, 2021, pp. 1743 - 1766. © 2021 The Japan Institute of Heterocyclic Chemistry
Received, 14th May, 2021, Accepted, 14th June, 2021, Published online, 17th June, 2021
DOI: 10.3987/COM-21-14496

NATURAL OSTHOLE-BASED ESTER DERIVATIVES AS POTENTIAL FUNGICIDAL AGENTS: DESIGN, SYNTHESIS AND QUANTITATIVE STRUCTURE-ACTIVITY RELATIONSHIP (QSAR)

Yong-Ling Wu,[1,2]* Yong Yan,[1] Tin-Tin Pan,[1,2] and Dou-dou Wang[1]

[1] College of Biology Pharmacy and Food Engineering, Shangluo University, Shangluo 726000, Shaanxi, China.
[2] Shaanxi Qinling Industrial Technology Research Institute of Special Biological Resources, Shangluo 726000, Shaanxi, China.
*Corresponding Author: Telephone +86-0914-2986016; fax +86-0914-2986016; E-Mail: wuyongling39@126.com

Abstract – Turning potential natural products into value-added fungicides is a bioactivity-guided mixed synthesis method. Thirty-two derivatives were designed and synthesized to improve the potential use of the osthole, a natural coumarin pharmacophore. Compound **Os14** with 3-ClPh showed a high *in vitro* and *in vivo* antifungal activity than other derivatives. The preliminary structure-activity relationships (SARs) demonstrated that compounds with a short aliphatic chain or electron-withdrawing groups on phenyl ring would have more desirable potency. Meanwhile, the quantitative structure-activity relationship (QSAR) model (R^2 = 0.928, F = 83.54, S^2 = 0.0042) were performed using Gaussian and CODESSA software with optimal conformers and heuristic regression analysis, which revealed a correlation of antifungal activity and molecular structures. Thus, these results laid the foundation for further design of improved crop-protection agents based on osthole scaffold.

INTRODUCTION

Emerging plant pathogens are increasingly recognized as a worldwide persistent threat to human and plant health which cause mortality and reduce fecundity of individual plants, meanwhile affect the structure and composition of natural plant communities.[1-3] What is worse, this threat is increasingly aggravated, not only due to plants and trees encountering new pathogens, but also global trade and transportation, climate changes, which were exaggerated this situation.[4] To the best of our knowledge,

diseases in crops cause major production and economic losses in agricultural industry worldwide.[5] Fortunately, chemical control has been critical in preventing losses from plant diseases, especially with the development of numerous specific-action fungicides.[6-8] However, residual toxicity, severe pesticide resistance, and environmental pollution detrimental effects with the commercial chemical fungicides expand were exacerbating.[9-11] Accordingly, there is a pressing need for the development of new, effective and safe agrochemicals for fungal diseases control in crops of sustainable agriculture.

Plant-derived natural products with environmental compatibilities, structural diversities and easy biodegradation have played an important role in drug discovery.[12-14] That is the reason why natural product have long been used as pesticides and has broadly served as a source of inspiration for a great many commercial synthetic pesticides that are in the market today.[15,16] In addition, discovering and screening antifungal candidates or scaffolds from thousands of natural products is virtually and economically impossible, while employing a bioactivity-guided mixed synthesis method would reduce the problems of cost and time requirements for screening.[17]

The dried fruit of *Cnidium monnieri* (L.) Cusson, a well-known traditional Chinese herb, possesses a variety of pharmacological properties and has been administered to humans in therapeutic applications for many years.[18] Osthole [7-methoxy-8-(3-methyl-2-butenyl)-2*H*-1-benzopyran-2-one] (Figure **1**) is an active compound isolated from the dried fruit of *Cnidium monnieri* (L.) Cusson. Osthole has raised considerable concern in medicinal and agricultural chemistry in recent years because of its diverse pharmacological and biological features, which make it a prospective natural lead compound for new drug discovery.[19,20] Actually, a great many natural or synthetic compounds containing osthole moiety showed important biological activities, such as anticancer,[21] antiinflammatory,[22] antiproliferative,[23] anticonvulsant,[24] and insecticidal[25] activity. Meanwhile, osthole derivatives also showed high activity against most of fungi.[26] Therefore, the bioactivity of osthole guided us to continue to seek new derivatives which with potent fungicidal efficacy.

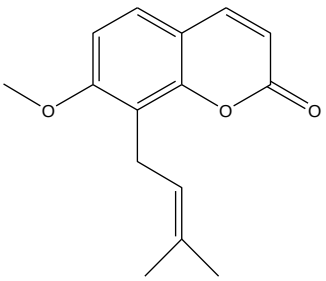

Figure 1. Chemical Structure of Osthole

In present study, we explored a concise approach to synthesize a collection of new ester-osthole derivatives by substituting with different electron groups of aromatic rings. Meanwhile, their antifungal

activity was tested. Since the *in vitro* antifungal activity of fungicides does not always match the *in vivo* activity, the *in vivo* activities were also tested. Moreover, structure-activity relationships (SAR) and quantitative structure-activity relationship (QSAR) model which was established via Codessa software were investigated to provide a helpful insight into further lead optimization.

RESULTS AND DISCUSSION

Chemistry. The intermediate compound **2** (7-hydroxyosthole) were obtained by Cys/NaH catalytic system under DMF solution through demethylation reaction. In order to investigate the structure-activity relationships, ester compounds **Os1-32** were synthesized by using dicyclohexylcarbodiimide (DCC) and catalytic dimethylaminopyridine (DMAP) in the coupling of carboxylic acids with compound **2** in 38%～68% yields. The structures of all the derivatives were characterized by ^{1}H NMR, ^{13}C NMR and high-resolution electrospray ionization mass spectrometry (HR-ESI-MS).

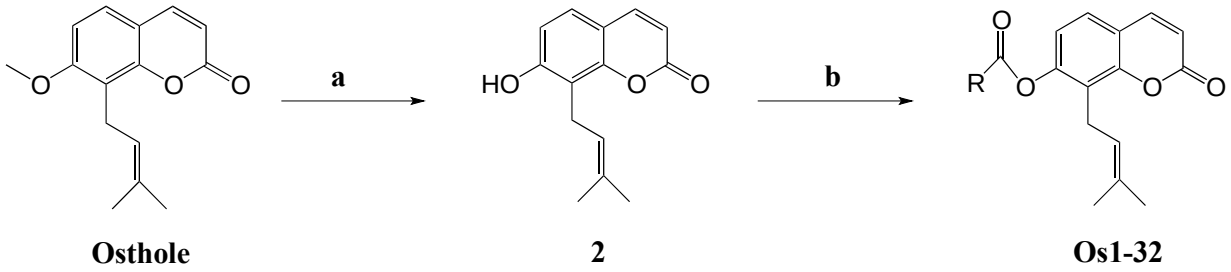

Osthole **2** **Os1-32**

Scheme 1. The synthetic routine to the target compounds **Os1-32**. Reagents and conditions: a) cysteine, NaH, osthole, DMF, 0 °C-80 °C: b) corresponding carboxylic acid, DMAP, DCC, CH_2Cl_2, 0 °C to rt.

Antifungal activity and SARs. The *in vitro* screening results of the title compounds for preliminary antifungal activities against seven pathogenic fungi (*Botrytis cinerea*, *Valsa mali* Miyabe et Yamada, *Alternaria brassicicola* (Schweinitz) Wilts., *Fusahum graminearum* Sehw., *Rhizoctonia solani*, *Colletotrichum gloeosporioides* Penz. *and Sclerotinia sclerotiorum*) at 100 μg/mL were listed in Table **1** and Figure **2**. The results showed most of the compounds exhibited certain to great inhibition activity against each of the fungi at 100 μg/mL. As shown therein, compound with *meta*-Cl of the phenyl group **Os14** was active against those seven fungi to various extent at the concentration of 100 μg/mL and exhibited the highest inhibitory activity against *Rhizoctonia solani* with inhibition ratio of 91.3%. Particularly, the antifungal activity of compounds **Os7, Os11, Os14, Os17**, and **Os31-32** were more potent than natural osthole. Furthermore, from the results we can see all the derivatives showed higher activity against *F. graminearum* Sehw. and *R. solani* than the other five pathogenic fungi generally.

Table 1. Initial Antifungal Activity of Compounds at 100 μg/mL

Compd.	average inhibition ratio (%) (100 μg/mL; 72 h)						
	B. c.	*V. m.*	*F. g.*	*R. s.*	*S. s.*	*A. b.*	*C. g.*
Os1	31.2 ± 1.2	22.2 ± 0.7	35.5 ± 1.2	32.7 ± 1.1	21.2 ± 0.5	10.7 ± 0.8	15.8 ± 1.2
Os2	42.5 ± 0.8	26.1 ± 0.4	38.3 ± 0.6	47.2 ± 0.4	32.3 ± 0.4	19.2 ± 1.3	17.6 ± 0.3
Os3	46.6 ± 0.5	32.4 ± 0.8	43.8 ± 0.8	58.6 ± 0.4	41.2 ± 0.8	31.7 ± 0.4	23.7 ± 0.4
Os4	57.9 ± 0.5	42.9 ± 1.2	62.9 ± 0.2	75.7 ± 0.3	59.4 ± 0.7	47.5 ± 0.7	41.7 ± 0.8
Os5	72.3 ± 1.3	58.4 ± 0.6	74.7 ± 1.3	81.8 ± 0.5	67.6 ± 0.3	58.5 ± 0.6	46.8 ± 0.6
Os6	60.6 ± 0.9	46.1 ± 0.5	61.2 ± 0.7	70.9 ± 0.3	52.7 ± 1.2	49.8 ± 0.5	37.2 ± 0.5
Os7	80.3 ± 0.7	65.4 ± 1.3	82.1 ± 1.5	89.3 ± 0.5	72.3 ± 0.3	63.9 ± 0.1	55.3 ± 0.2
Os8	67.4 ± 0.5	51.8 ± 0.2	68.3 ± 0.6	72.2 ± 1.1	60.7 ± 0.6	52.0 ± 0.2	44.2 ± 0.1
Os9	72.5 ± 0.6	55.4 ± 0.5	76.2 ± 0.4	80.1 ± 0.9	65.8 ± 0.4	55.3 ± 0.5	49.1 ± 0.7
Os10	79.8 ± 0.4	61.1 ± 0.2	81.2 ± 0.5	84.6 ± 0.1	68.6 ± 0.1	58.5 ± 0.2	51.5 ± 0.3
Os11	84.3 ± 0.2	64.5 ± 0.2	85.3 ± 0.8	90.6 ± 0.3	72.5 ± 0.2	63.0 ± 0.6	54.6 ± 0.3
Os12	75.6 ± 0.8	56.4 ± 0.6	78.2 ± 0.6	80.4 ± 0.5	65.4 ± 0.6	56.4 ± 0.8	48.6 ± 0.6
Os13	82.1 ± 0.2	63.2 ± 0.4	83.1 ± 0.8	85.6 ± 0.8	69.8 ± 0.9	62.2 ± 0.7	50.3 ± 0.5
Os14	89.3 ± 0.9	66.6 ± 0.3	90.4 ± 0.7	91.3 ± 0.9	78.2 ± 0.5	67.5 ± 0.1	55.2 ± 0.6
Os15	77.0 ± 0.8	60.5 ± 0.4	78.7 ± 0.1	82.4 ± 0.4	63.6 ± 0.8	59.5 ± 0.6	47.4 ± 0.8
Os16	76.4 ± 0.6	58.2 ± 0.3	79.0 ± 0.8	82.3 ± 0.5	66.2 ± 0.1	58.2 ± 0.8	50.1 ± 0.9
Os17	78.3 ± 0.7	60.4 ± 0.9	82.4 ± 1.6	88.2 ± 2.1	69.2 ± 0.4	60.4 ± 0.7	53.2 ± 0.7
Os18	73.4 ± 0.2	56.8 ± 0.7	76.7 ± 0.2	79.3 ± 0.6	65.3 ± 0.6	56.5 ± 0.2	48.8 ± 0.5
Os19	74.6 ± 0.8	56.4 ± 0.5	77.9 ± 0.1	81.3 ± 0.5	65.7 ± 0.2	56.1 ± 0.6	49.3 ± 0.6
Os20	75.8 ± 0.5	56.6 ± 0.8	78.5 ± 0.6	83.7 ± 0.2	68.3 ± 0.5	58.5 ± 0.5	51.5 ± 0.7
Os21	72.3 ± 0.1	55.2 ± 0.3	75.4 ± 0.7	78.1 ± 0.4	61.8 ± 0.2	54.4 ± 0.3	47.2 ± 0.9
Os22	67.4 ± 0.7	51.6 ± 0.2	71.4 ± 0.6	72.2 ± 0.4	60.2 ± 0.6	52.4 ± 0.4	48.4 ± 0.5
Os23	70.2 ± 0.5	54.3 ± 0.5	72.3 ± 0.2	76.0 ± 0.5	63.3 ± 0.2	54.7 ± 0.2	50.1 ± 0.8
Os24	64.2 ± 0.1	48.2 ± 0.7	67.5 ± 0.6	70.7 ± 0.4	58.3 ± 0.6	49.6 ± 0.1	45.6 ± 0.2
Os25	65.6 ± 0.5	48.1 ± 0.6	68.4 ± 0.3	69.2 ± 0.2	57.2 ± 0.8	50.3 ± 0.5	46.4 ± 0.2
Os26	67.4 ± 0.3	51.8 ± 0.3	70.5 ± 0.5	72.4 ± 0.2	60.4 ± 0.2	52.6 ± 0.3	49.5 ± 0.7
Os27	62.2 ± 0.7	45.4 ± 0.7	64.7 ± 0.8	67.1 ± 0.6	54.5 ± 0.1	46.2 ± 0.4	40.2 ± 0.1
Os28	60.1 ± 0.3	44.5 ± 0.5	65.3 ± 0.9	62.8 ± 0.9	52.6 ± 0.4	52.1 ± 0.5	41.5 ± 0.2
Os29	62.0 ± 0.5	46.7 ± 0.5	66.5 ± 0.6	67.6 ± 0.4	56.2 ± 0.5	57.4 ± 0.7	44.6 ± 0.8
Os30	57.3 ± 0.2	42.2 ± 0.3	61.4 ± 0.4	58.5 ± 0.7	48.6 ± 0.2	47.6 ± 0.4	40.6 ± 0.3
Os31	78.1 ± 0.6	58.6 ± 0.6	84.2 ± 0.3	89.2 ± 0.1	70.3 ± 0.1	62.3 ± 0.2	50.3 ± 0.2
Os32	72.4 ± 0.5	55.2 ± 1.1	79.1 ± 0.5	82.8 ± 0.5	66.4 ± 0.5	58.9 ± 0.5	48.5 ± 0.6
Osthole	78.2 ± 1.2	53.5 ± 1.7	81.3 ± 0.2	88.3 ± 0.4	65.8 ± 1.1	51.1 ± 0.9	45.3 ± 0.5

B. c.: Botrytis cinerea, V. m.: Valsa mali Miyabe et Yamada, *F. g.: Fusarium graminearum* Sehw., *R. s.: Rhizoctonia solani, S. s.: Sclerotinia sclerotiorum, A. b.: Alternaria brassicicola* (Schweinitz) Wilts., *C. g.: Colletotrichum gloeosporioides* Penz.

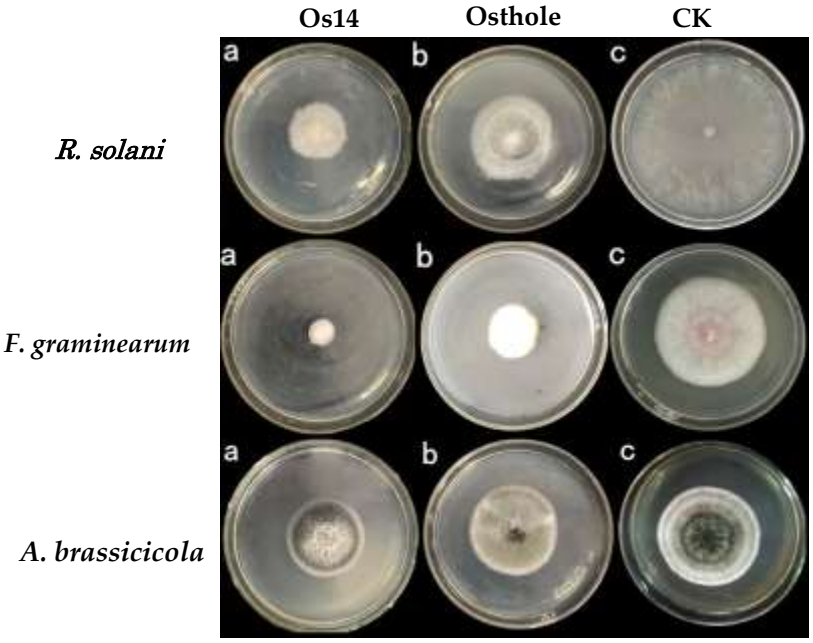

Figure 2. *In vitro* antifungal activity of compounds against *Rhizoctonia solani*, *Fusarium graminearum* and *Alternaria brassicicola* (Schweinitz) Wilts. at 100 μg/mL, CK is a blank control with 0.25% DMSO

Table 2. *In vitro* fungicidal activity of compounds against *Fusarium graminearum* Sehw. *and Rhizoctonia solani* [a]

Compd.			*F. graminearum* Sehw.	*R. solani*	
No.		R	IC_{50}, μM	IC_{50}, μM	pIC_{50}[c]
1.	**Os1**	H	124.5 ± 8.7	113.6 ± 6.5	-2.06
2.	**Os2**	Me	102.3 ± 5.9	99.7 ± 4.3	-2.00
3.	**Os3**	Et	77.6 ± 6.3	52.2 ± 3.6	-1.72
4.	**Os4**	$Me(CH_2)_2$	45.1 ± 3.5	33.5 ± 1.7	-1.53
5.	**Os5**	$Me(CH_2)_3$	28.5 ± 2.6	13.6 ± 2.4	-1.13
6.	**Os6**	$(Me)_2CHCH_2$	41.4 ± 1.1	25.7 ± 3.3	-1.41
7.	**Os7**	$Me(CH_2)_4$	22.7 ± 2.2	10.8 ± 3.6	-1.03
8.	**Os8**	$(Me)_2CHCH_2CH_2$	32.8 ± 0.9	19.9 ± 3.2	-1.30
9.	**Os9**	C_6H_5	42.3 ± 1.4	27.8 ± 2.1	-1.44
10.	**Os10**	2-FC_6H_4	28.5 ± 2.3	17.2 ± 1.8	-1.24
11.	**Os11**	3-FC_6H_4	22.7 ± 2.1	12.6 ± 0.6	-1.10
12.	**Os12**	4-FC_6H_4	34.1 ± 1.6	19.4 ± 1.1	-1.29
13.	**Os13**	2-ClC_6H_4	24.6 ± 0.2	12.3 ± 0.5	-1.09
14.	**Os14**	3-ClC_6H_4	17.2 ± 1.4	8.7 ± 1.7	-0.94
15.	**Os15**	4-ClC_6H_4	29.4 ± 1.8	16.7 ± 1.6	-1.22
16.	**Os16**	2-BrC_6H_4	28.7 ± 2.2	20.4 ± 1.2	-1.31
17.	**Os17**	3-BrC_6H_4	26.4 ± 1.6	17.3 ± 0.4	-1.24

18.	**Os18**	4-BrC_6H_4	36.8 ± 3.4	25.1 ± 2.3	-1.40
19.	**Os19**	2-CNC_6H_4	37.6 ± 2.6	28.5 ± 2.1	-1.45
20.	**Os20**	3-CNC_6H_4	31.5 ± 2.4	21.3 ± 1.7	-1.33
21.	**Os21**	4-CNC_6H_4	40.7 ± 3.3	29.1 ± 3.5	-1.46
22.	**Os22**	2-MeC_6H_4	53.6 ± 2.4	36.8 ± 4.5	-1.57
23.	**Os23**	3-MeC_6H_4	48.5 ± 2.3	30.5 ± 1.8	-1.48
24.	**Os24**	4-MeC_6H_4	60.4 ± 1.7	45.7 ± 3.6	-1.66
25.	**Os25**	2-$MeOC_6H_4$	61.2 ± 2.8	53.3 ± 3.2	-1.73
26.	**Os26**	3-$MeOC_6H_4$	52.1 ± 1.6	50.5 ± 2.7	-1.70
27.	**Os27**	4-$MeOC_6H_4$	68.8 ± 2.7	59.6 ± 2.1	-1.78
28.	**Os28**	2-HOC_6H_4	77.9 ± 3.5	61.4 ± 3.2	-1.79
29.	**Os29**	3-HOC_6H_4	69.6 ± 2.3	56.3 ± 4.5	-1.75
30.	**Os30**	4-HOC_6H_4	82.5 ± 2.2	63.7 ± 2.1	-1.80
31.	**Os31**	2,4-$Cl_2C_6H_3$	24.6 ± 0.4	11.2 ± 1.6	-1.05
32.	**Os32**	3,5-$F_2C_6H_3$	29.5 ± 1.3	15.8 ± 0.7	-1.20
33.	**Osthole** [b]		24.2 ± 1.4	9.3 ± 0.6	-
34.	**Carbendazim** [b]		8.2 ± 0.8	2.7 ± 0.4	-

[a] All half maximal inhibitory concentration (IC_{50}) values are presented as the means ± SD (n = 3), μM. [b] Osthole and carbendazim was used as the positive control. [c] pIC_{50}, the tested IC_{50} values were converted into the corresponding plog IC_{50} values.

According to these preliminary results, the half maximal inhibitory concentration (IC_{50}) of all the derivatives against *F. graminearum* Sehw. *and R. solani* were tested by the mycelial growth inhibitory rate method. We first investigated the influence of variations of ester alkyl chain length on the antifungal activity, and results were summarized in Table **2**, we can see derivatives **Os5** and **Os7** increasing the chain length to four and five carbons displayed a superior activity against *F. graminearum* Sehw. (IC_{50} = 28.5, 22.7 μM) than the derivatives **Os1-4** (IC_{50} = 45.1-124.5 μM) which the number of carbons were less than or equal to three. Meanwhile, the bulky group with branching chains of derivatives **Os6** and **Os8** conferred a dramatic potency decrease. These results indicate that branched alkyl groups with larger volumes and shapes may interfere with receptor binding. Secondly, further SAR studies of electron-withdrawing or electron-donating groups on the phenyl ring were performed. Initial attempts to introduce no substituent on the phenyl group of **Os9** (IC_{50} = 42.3 μM against *F. graminearum* Sehw.) led to a less active than natural products osthole (IC_{50} = 24.2 μM). A more potent activities were observed when substitution of halogen atoms F, Cl, Br and CN electron-withdrawing group at the *para*-, *meta*-, and *ortho*-position were installed into phenyl group. As it can be seen that compound **Os14** with 3-ClPh showed a high activity against *F. graminearum* Sehw. (IC_{50} = 17.2 μM) compared to osthole. In contrast,

the electron-donating groups of Me, MeO, and OH on the phenyl group were made no contribution to improving the potency in the case of **Os22-30** (IC_{50} = 31.5-82.5 μM).

Particularly, derivatives **Os28-30**, the hydroxyl substitution resulted in a significant loss of inhibitory activity, which suggesting the hydroxyl group is disfavored. As we can see, the steric effect also played an essential role for the antifungal activity. When the substituent was shifted from the *meta*-position to the *ortho*- or *para*-position, a considerable decrease in potency was observed. Additionally, we explored whether incorporating simultaneously two halogen atoms would provide synergistic effect. Somewhat unexpectedly, we observed that the disubstituted compounds **Os31** and **Os32** were less potent than the related monosubstituted analogue **Os14** and **Os11**. On the whole, these results demonstrated that the *meta*-position of the phenyl ring derivatives could tolerate both electron-donating and electron-withdrawing groups much better than the *para*- or *meta*-position, and confirmed the importance of substituents on the *meta*-position with proper size or the electron-withdrawing characteristic. Summarizing, new structure-activity relationship (SAR) studies on ester compounds of osthole allowed their antifungal activity to be attributed to two factors: benzopyrone and isoamylene, which are essential; and a short aliphatic chain and electron-withdrawing groups, which improve antifungal activity. Graphical depiction of the general SAR for antifungal activity based on the IC_{50} results on *F. graminearum* Sehw. was shown in Figure **3**.

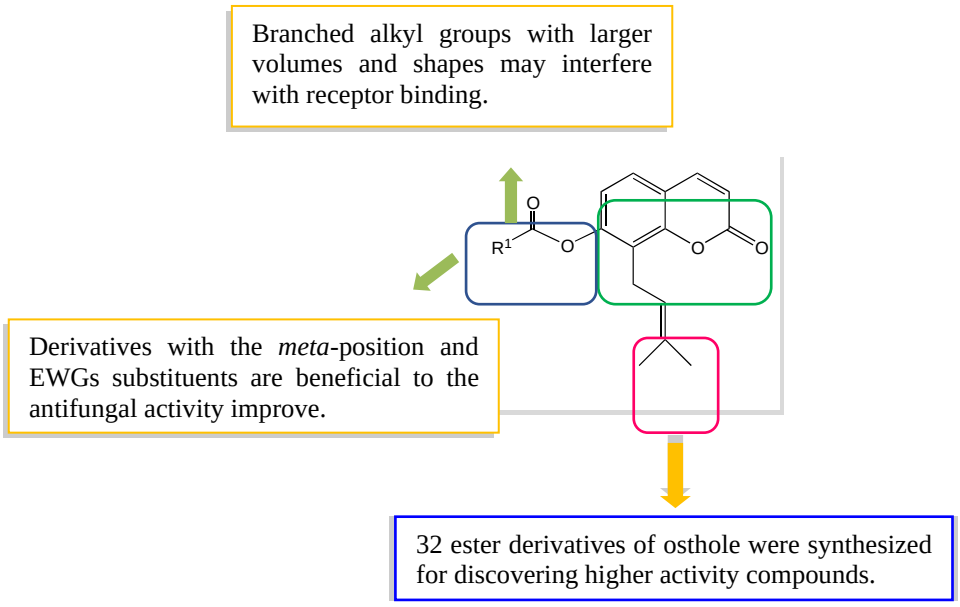

Figure 3. Graphical depiction of the general SAR for antifungal activity based on the IC_{50} results on *F. graminearum* Sehw.; EWGs: electron-withdrawing groups.

***In vivo* fungicidal bioactivity.** In order to further confirm the antifungal activity of title compounds, the *in vivo* fungicidal activities (protective effect) of the 12 promising derivatives were tested against *B. cinerea* on tomato fruits, which were washed thoroughly with sterile water, then spray tested samples until liquid flowed on surface before inoculation, after 3 days, the average lesion diameter and the disease control efficacy was calculated. Against *B. graminis* on wheat seedlings, spray the tested samples uniform on the desired wheat leaves 24 h before shaking spores, after inoculated 7 days, calculate the biocontrol effect. As can be seen in Table 3 and Figure 4, compound **Os14** showed great activity which preventatives inhibit rates were higher than 70% equivalent with natural products osthole. Particularly, the inhibit rates of compound **Os14** against *B. graminis* was equal with commercial fungicide triadimefon. Taken together, *in vivo* fungicidal activities of derivatives in this research were aligned with *in vitro* activities.

Table 3. *In vivo* fungicidal activity (protective effect) of compounds against *B. cinerea*, and *B. graminis* (250 μg/mL)

Compounds			against *B. cinerea* (%)	against *B. graminis* (%)
	No.	R		
1.	**Os1**	H	26.13	34.71
2.	**Os4**	$Me(CH_2)_2$	38.45	49.62
3.	**Os8**	$(Me)_2CHCH_2CH_2$	55.62	63.13
4.	**Os9**	C_6H_5	50.21	62.54
5.	**Os11**	3-FC_6H_4	68.23	75.61
6.	**Os14**	3-ClC_6H_4	74.76	84.25
7.	**Os17**	3-BrC_6H_4	52.64	62.43
8.	**Os20**	3-CNC_6H_4	48.22	50.87
9.	**Os23**	3-MeC_6H_4	45.13	42.23
10.	**Os29**	3-HOC_6H_4	32.34	33.45
11.	**Os31**	2,4-$Cl_2C_6H_3$	67.65	76.21
12.	**Os32**	3,5-$F_2C_6H_3$	54.82	68.62
13.	**Osthole**		72.43	83.24
14.	**Triadimefon**		-	82.16
15.	**Carbendazim**		88.52	-

Values are means of three replicates; Commercial fungicide, triadimefon and carbendazim were used as the positive control.

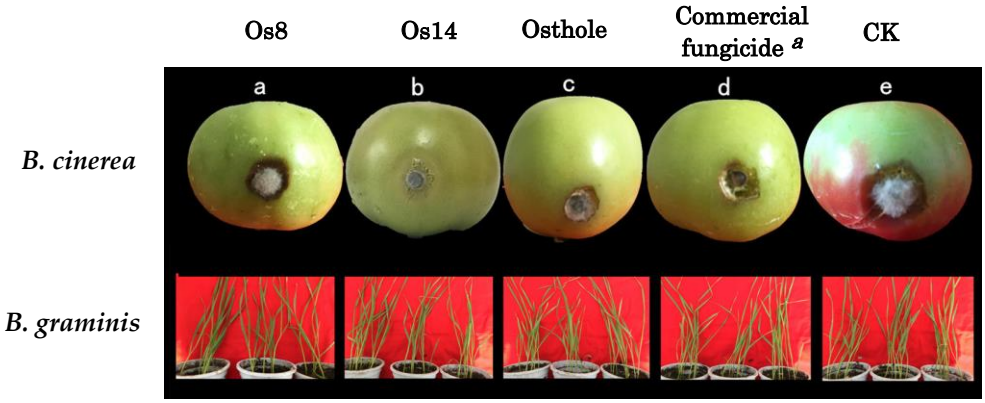

Figure 4. *In vivo* antifungal activity of compounds against *Botrytis cinereal* and *Blumeria graminis* at 250 μg/mL. [a] Commercial fungicide, carbendazim was used as the *B. cinerea* positive control, triadimefon was used as the *B. graminis* positive control.

QSAR study and antifungal activity against *B. cinerea*. The conformers optimize and minimum energy calculation was an essential procedure in construction of QSAR model. In view of the number of samples and descriptors used in this study, the heuristic regression was selected for developing the QSAR model which with satisfactory values of R^2, F, and S^2.

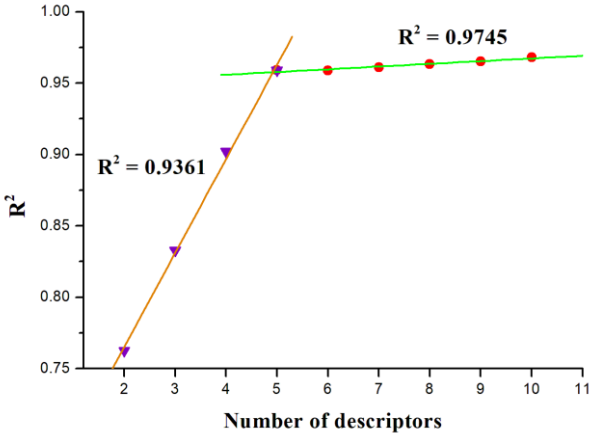

Figure 5. The "breaking point" rule results

The number of descriptors was achieved by the "breaking point" rule, as described in Figure **5**, the R^2 value of the heuristic regression had a dramatic increase before the number of the descriptors reached 5, descriptors with high t values were accepted and those with low t values were rejected. After the number of the descriptors reached a certain value, the improvement of the regression model became less insignificant ($\triangle R^2$ < 0.02-0.04). Meanwhile, the numbers of samples and descriptors also meet the

equation (3D ≤ S-3, S means the number of samples; D means the number of descriptors). At last, the final 5-descriptor model was generated. In the Supplementary Information, the five significant descriptors and values are listed.

The five descriptor QSAR model equation was shown in Table **4**. According to this optimaized model, the comparison chart of predictive and practical activity of 32 compounds was exhibited in Figure **6**. Compared with experimental pIC_{50} (negative log IC_{50}), we could conclude that the generated model was reliable. The final QSAR model with 5 descriptors was shown in as

$$pIC_{50} = -2.3562 + 6.8914 \times \text{Total charge} + 5.2356 \times q^{O}_{max} - 2.4761 \times n_o - 0.9235 \times q^{C}_{min} + 1.5734 \times \mu_h$$

$$N = 32,\ R^2 = 0.928,\ F = 83.54,\ S^2 = 0.0042$$

Table 4. The best five-descriptor model

Descriptor No.	*X*	±△*X*	*t*-Text	Descriptor
0	-2.3562	4.2742×10^{-1}	4.5563	Intercept
1	6.8914	3.5398×10^{-1}	-6.8094	Total charge [a]
2	5.2356	9.3023	-10.6702	q^{O}_{max} [b]
3	-2.4761	4.0921	5.5513	n_o [c]
4	-9.235×10^{-1}	2.7352×10^{-2}	-3.5762	q^{C}_{min} [d]
5	1.5734	4.1254×10^{-1}	2.7423	μ_h [e]

[a] Total charge of the substituent groups on the osthole-based backbone structure. [b] Max. net atomic charge for an O atom. [c] Number of occupied electronic levels of atoms. [d] Minimum net atomic charge for a C atom. [e] Tot hybridization composite of the molecular dipole.

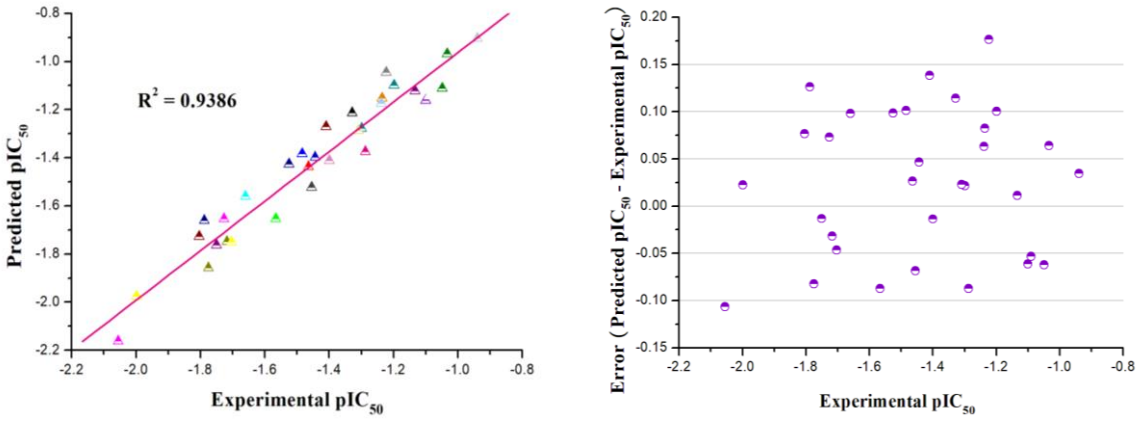

Figure 6. Experimental pIC_{50} *versus* predicted pIC_{50} and pIC_{50} values *versus* respective errors

The internal validation and the "leave-one-out" cross-validation methods were carried out to validate of the established QSAR model.[27] Internal validation results are presented in Supplementary Information. The $R^2_{Training}$ and R^2_{Test} are within 5% for all three sets, and the average values of $R^2_{Training}$ and R^2_{Test} were approach the overall R^2 value. So, the obtained QSAR model indicated the predictive power of 3-fold cross-validation. In the "leave-one-out" method, as can be seen in table **5**, every fourth compounds were an external test set, and the others were the training set. The R^2 value of the training set and test set were close, and the QSAR model acquired in this study was available.

Table 5. Internal validation of the QSAR model [a]

Training set	*N*	R^2	*F*	S^2	Test set	*N*	R^2	*F*	S^2
A+B	22	0.924	85.71	0.0041	C	10	0.935	84.16	0.0046
B+C	21	0.936	83.35	0.0049	A	11	0.942	85.35	0.0041
A+C	21	0.929	85.24	0.0045	B	11	0.923	82.54	0.0042
Average		0.930	84.77	0.0045	Average		0.933	84.02	0.0043

[a] Compds. A: 1, 4, 7, 10, 13, 16, 19, 22, 25, 28, 31. Compds. B: 2, 5, 8, 11, 14, 17, 20, 23, 26, 29, 32. Compds. C: 3, 6, 9, 12, 15, 18, 21, 24, 27, 30.

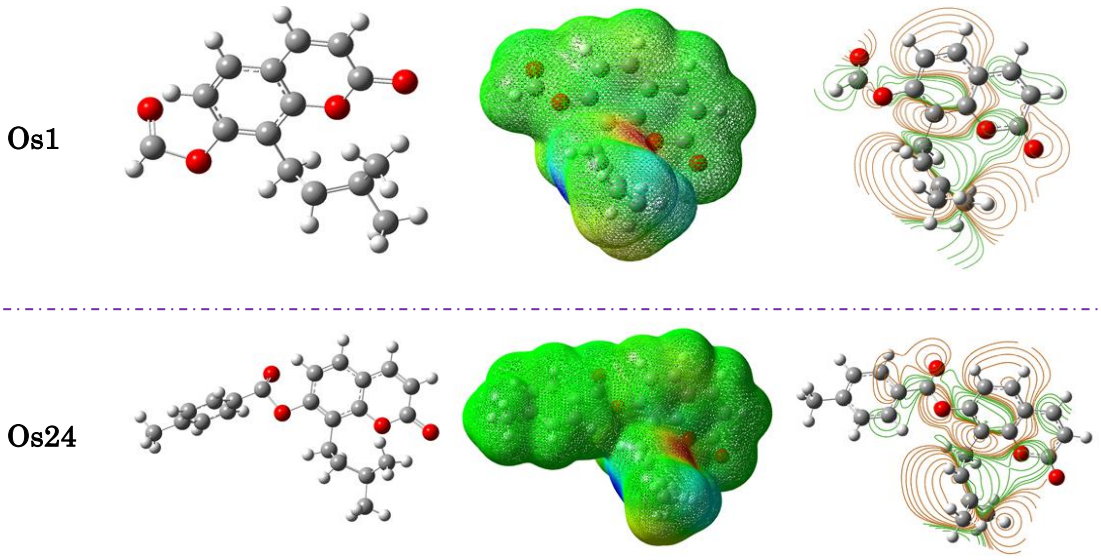

Figure 7. Molecular electrostatic potential and contour maps of compounds **Os1** and **Os24**. The green parts represent positive molecular orbitals, and the red parts represent negative molecular orbitals.

To the molecular descriptors, the first important descriptor was total charge of the substituent groups on the osthole-based backbone structure which is an electrostatic descriptor. This descriptor was essential for

modulating the antifungal activity against *Rhizoctonia solani* because of the presence of carbon-oxygen double bond and carbon-carbon double bond. As the presence of electro activity difference between the atoms, the permanent polarization was shown in the molecular electrostatic potential map (Figure **7**).[28-30] Therefore, the C=O and C=C atoms may bind with plants cells present at the target site. Meanwhile, the contour maps of the title compounds revealed the higher electron density around the substituent groups on the oxygen atoms of osthole-based backbone structure is contribute to the antifungal activity (Figure **7**). These effects suggested that the electrostatic properties of oxygen atom were an integral element in the design of potential fungicides as they directly affect the activity.

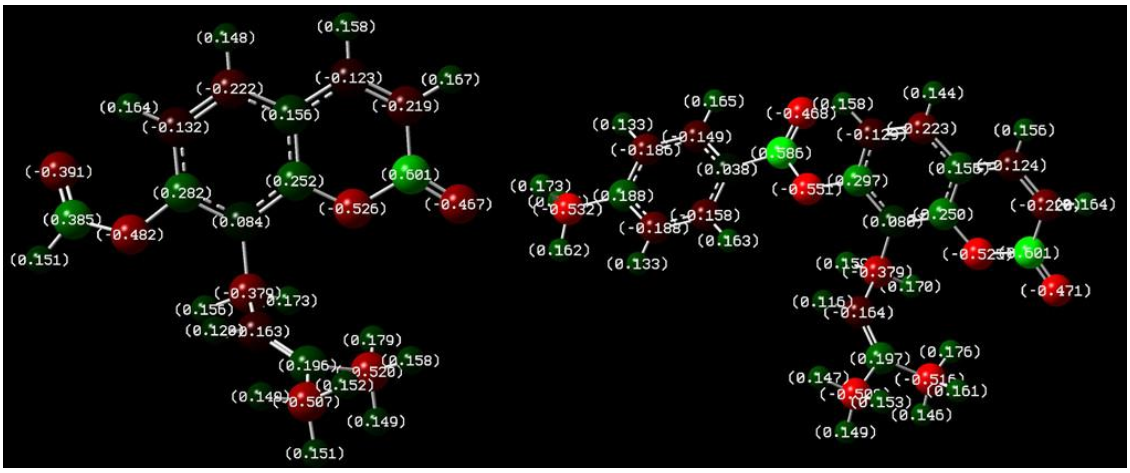

Figure 8. Optimized geometries and charge distribution of compounds **Os1** and **Os24**

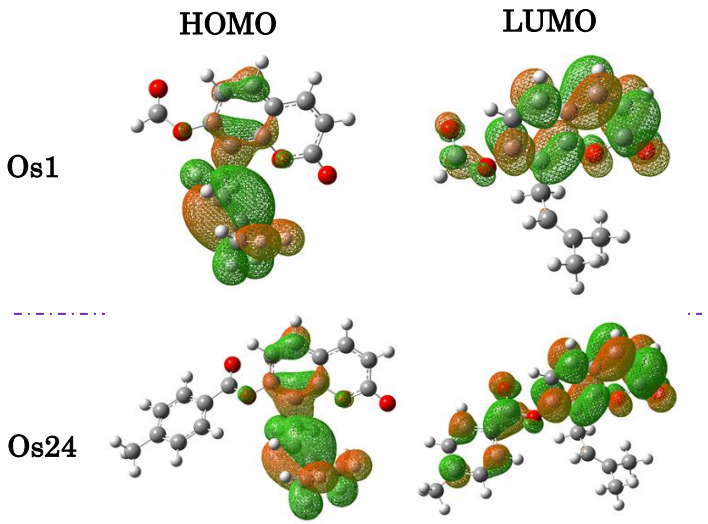

Figure 9. Ground state isodensity surface plots for molecular orbitals compounds **Os1** and **Os24**

The maximum net atomic charge for an O atom and minimum net atomic charge for a C atom were the third and fourth important descriptors as described in Table **4**. Atomic charges or local electron densities

has been widely used to interpret the chemical reactivity and physicochemical properties of molecules,[31,32] the atomic charges are also electrostatic descriptors and reflect the charge distribution of the molecules as shown in the optimized geometries maps of compounds **Os1** and **Os24** (Figure **8**). Figure **9** showed the frontier molecular orbitals (FMOs) of compounds **Os1** and **Os24**, which indicated the highest occupied molecular orbital (HOMO) and the lowest unoccupied molecular orbital (LUMO).[33] These quantum-chemical parameters could determine the molecular chemical reactivity and the ability of electron transport.

The 3rd and 5th descriptors obtained in the model were the number of occupied electronic levels of atoms and tot hybridization composite of the molecular dipole. These two descriptors belong to quantum-chemically descriptors and reflect the quantitative measure of the lipophilic and hydrophobic properties of the compounds. An appropriate μ_h value illustrated that the molecules can penetrate fungi cell membrane or wall more smoothly as well as interact with the action target. And the number of occupied electronic levels of atoms which could describes the molecules polar interactions and calculated charge distribution in the molecules.[34-36]

CONCLUSION

In this study, 32 ester derivatives based osthole, namely, **Os1-32**, were synthesized, and their antifungal activity were investigated. Bioassay results indicated that osthole derivatives had higher activity against *F. graminearum* Sehw. and *R. solani* than the other five pathogenic fungi generally. Particularly, compound **Os14** with 3-ClPh showed a high activity against *F. graminearum* Sehw.. The SAR indicated that a short aliphatic chain or electron-withdrawing groups on phenyl ring possessed superior activity over the electron-donating groups derivatives. Moreover, the QSAR study indicated that total charge of the substituent groups on the osthole-based backbone structure, max. net atomic charge for an O atom and tot hybridization composite of the molecular dipole played a beneficial effect on the antifungal activity. Taken together, these results laid the foundation for the design of new fungicides based on the scaffold osthole.

EXPERIMENTAL

General Information. Carbendazim and triadimefon, purchased from Xiangtan Huayuan Fine-Chem Co. Ltd. (Xiangtan, China). Osthole, cysteine (Cys), 4-dimethylaminopyridine (DMAP), *N*,*N*-dicyclohexylcarbodiimide (DCC), carboxylic acids and other chemicals were all purchased from Aladdin Industrial Inc. (Shanghai, China). All solvents were analytical grade and directly used, unless otherwise noted. All solvents were dried, and redistilled before use. The water used was redistilled and ion-free. Analytical thin-layer chromatography (TLC) was performed on silica gel GF254. Column

chromatographic (CC) purification was carried out using silica gel (200-300 mesh). Above silica gel was obtained from Qingdao Haiyang Chemical Co., Ltd. (Qingdao, China). The melting points of these synthetic derivatives were determined on an X-6 apparatus and uncorrected, which was bought from Beijing Tech. Nuclear magnetic resonance spectra (NMR) were performed on Bruker Avance 500 MHz instrument. HR-MS (ESI) was obtained using a Bruker Apex-Ultra 7.0 T spectrometer. Reaction progress was monitored by thin-layer chromatography on silica gel GF-254 with detection by UV light.

Synthetic Procedures. General Synthetic Procedure for the Intermediate Compounds

As shown in Scheme 1, cysteine (10 mmol), sodium hydride (NaH, 60% dispersion in mineral oil) (20 mmol) were added to dimethylformamide (DMF) (100 mL) and stirred at room temperature for 1 h. After that, osthole (5 mmol) was added and the reaction mixture was heated to 80 °C for 3 h. TLC was used to monitor whether the reaction was completed. After cooling, 10% HCl was added to the above mixture to make it acidic. The resulting yellow liquid was then extracted with EtOAc, and washed with water for 3 times, dried over Na_2SO_4, and evaporated. The crude product was purified by column chromatography with petroleum ether-EtOAc (10:3) to afford compound **2** as a white solid.

General Synthetic Procedure for Ester Compounds. 4-Dimethylaminopyridine (DMAP, 0.1 mmol) and intermediate compounds **2** (1.0 mmol) were added to the anhydrous CH_2Cl_2 (15.0 mL) of the respective carboxylic acid (1.2 mmol). Then the mixture was cooled to 0 °C. *N*, *N*-Dicyclohexylcarbodiimide (DCC, 226.0 mg, 1.1 mmol) dissolved in the anhydrous CH_2Cl_2 (20.0 mL) which was added dropwise into the mixture over a period of 0.5 h at 0 °C and then stirred at the room temperature. Then, filter the mixture. Finally, the residual organic layers were extracted by EtOAc (3×30 mL) and dried over anhydrous Na_2SO_4. After filtered, the solution was evaporated under vacuum. The target compounds were purified by column chromatography (petroleum ether/EtOAc = 5:1) to obtian the pure products **Os1-32** (Scheme **1**).[37] The structures of all ester derivatives were characterized by ^{1}H NMR, ^{13}C NMR, and HR-ESI-MS, and the data are listed below.

7-Hydroxy-8-prenylcoumarin (2). White crystals mp 96.3-97.1 °C; 82% yield; ^{1}H NMR (500 MHz, $CDCl_3$): δ 7.88 (d, *J* = 9.2 Hz, 1H), 7.35 (d, *J* = 8.4 Hz, 1H), 6.87 (d, *J* = 8.4 Hz, 1H), 6.25 (d, *J* = 9.2 Hz, 1H), 5.18 (t, *J* = 7.2 Hz, 1H), 3.37 (d, *J* = 5.2 Hz, 2H), 1.78 (s, 3H), 1.62 (s, 3H). ^{13}C NMR (125 MHz, $CDCl_3$): δ 162.0, 158.4, 153.0, 144.4, 135.8, 126.6, 120.3, 114.8, 113.2, 112.6, 112.2, 25.8, 22.0, 18.0. HR-MS (ESI): *m/z* calcd for $C_{14}H_{14}O_3$ ($[M + H]^+$) 231.1018, found 231.1019.

(7-Formyloxy-8-isoprenyl)coumarin (Os1). White crystals; mp 112.3-112.9 °C; 55% yield; ^{1}H NMR (500 MHz, $CDCl_3$): δ 7.88 (d, *J* = 9.2 Hz, 1H), 7.42 (d, *J* = 8.1 Hz, 1H), 6.91 (d, *J* = 7.8 Hz, 1H), 6.47 (d, *J* = 9.2 Hz, 1H), 5.82 (t, *J* = 7.2 Hz, 1H), 3.24 (d, *J* = 7.2 Hz, 2H), 1.81 (s, 3H), 1.65 (s, 3H). ^{13}C NMR

(125 MHz, $CDCl_3$): δ 162.0, 158.6, 153.4, 151.9, 144.4, 135.8, 125.1, 124.5, 120.7, 115.2, 112.6, 112.2, 25.8, 22.1, 18.2. HR-MS (ESI): *m/z* calcd for $C_{15}H_{14}O_4$ ($[M + H]^+$) 259.0956, found 259.0954.

(7-Acetoxy-8-isoprenyl)coumarin (Os2). White crystals; mp 111.5-112.2 °C; 53% yield; ^{1}H NMR (500 MHz, $CDCl_3$): δ 7.82 (d, *J* = 9.2 Hz, 1H), 7.41 (d, *J* = 8.2 Hz, 1H), 6.91 (d, *J* = 7.8 Hz, 1H), 6.42 (d, *J* = 9.2 Hz, 1H), 5.80 (t, *J* = 7.2 Hz, 1H), 3.22 (d, *J* = 7.2 Hz, 2H), 2.08 (s, 3H), 1.81 (s, 3H), 1.62 (s, 3H). ^{13}C NMR (100 MHz, $CDCl_3$): δ 168.2, 162.0, 153.4, 151.9, 145.6, 134.7, 124.5, 124.0, 123.4, 118.0, 117.9, 116.9, 25.3, 19.3, 16.9, 12.4. HR-MS (ESI): *m/z* calcd for $C_{16}H_{17}O_4$ ($[M + H]^+$) 273.1122, found 273.1123.

(7-Propionyloxy-8-isoprenyl)coumarin (Os3). White crystals; mp 114.7-115.3 °C; 52% yield; ^{1}H NMR (500 MHz, $CDCl_3$): δ 7.78 (d, *J* = 9.1 Hz, 1H), 7.39 (d, *J* = 8.4 Hz, 1H), 6.91 (d, *J* = 7.8 Hz, 1H), 6.43 (d, *J* = 9.2 Hz, 1H), 5.82 (t, *J* = 7.2 Hz, 1H), 3.34 (d, *J* = 7.2 Hz, 2H), 2.27 (q, *J* = 7.5 Hz, 2H), 1.83 (s, 3H), 1.63 (s, 3H), 1.02 (t, *J* = 7.5 Hz, 3H). ^{13}C NMR (125 MHz, $CDCl_3$): δ 169.0, 162.0, 153.4, 151.9, 145.4, 134.8, 124.9, 124.0, 123.4, 118.2, 117.9, 116.9, 25.4, 19.5, 16.9, 12.3, 9.1. HR-MS (ESI): *m/z* calcd for $C_{17}H_{18}NaO_4$ ($[M + Na]^+$) 309.1097, found 309.1097.

(7-Butyryloxy-8-isoprenyl)coumarin (Os4). White crystals; mp 116.8-117.5 °C; 56% yield; ^{1}H NMR (500 MHz, $CDCl_3$): δ 7.87 (d, *J* = 9.2 Hz, 1H), 7.41 (d, *J* = 8.2 Hz, 1H), 6.95 (d, *J* = 7.8 Hz, 1H), 6.48 (d, *J* = 9.2 Hz, 1H), 5.84 (t, *J* = 7.2 Hz, 1H), 3.27 (d, *J* = 7.2 Hz, 2H), 2.23-2.31 (m, 2H), 1.88 (s, 3H), 1.65 (s, 3H), 1.57 (dt, *J* = 14.5 Hz, 2H), 0.96 (t, *J* = 7.5 Hz, 3H). ^{13}C NMR (125 MHz, $CDCl_3$): δ 169.0, 161.8, 153.5, 151.6, 145.4, 134.8, 124.9, 124.0, 123.4, 118.2, 117.9, 116.9, 35.5, 25.3, 19.3, 18.2, 13.3, 12.4. HR-MS (ESI): *m/z* calcd for $C_{18}H_{20}NaO_4$ ($[M + Na]^+$) 323.1254, found 323.1255.

(7-Valeryloxy-8-isoprenyl)coumarin (Os5). White crystals; mp 118.9-119.6 °C; 43% yield; ^{1}H NMR (500 MHz, $CDCl_3$): δ 7.88 (d, *J* = 9.2 Hz, 1H), 7.43 (d, *J* = 8.1 Hz, 1H), 6.88 (d, *J* = 7.8 Hz, 1H), 6.28 (d, *J* = 9.2 Hz, 1H), 5.26 (t, *J* = 7.4 Hz, 1H), 3.48 (d, *J* = 7.2 Hz, 2H), 2.23-2.31 (m, 2H), 1.78 (s, 3H), 1.65 (s, 3H), 1.52 (t, *J* = 7.8 Hz, 2H), 1.31 (dt, *J* = 14.5 Hz, 2H), 0.91 (t, *J* = 7.1 Hz, 3H). ^{13}C NMR (125 MHz, $CDCl_3$): δ 169.0, 161.8, 153.5, 151.6, 145.4, 134.8, 124.5, 124.0, 123.4, 118.2, 117.9, 116.9, 32.9, 27.6, 25.3, 22.5, 19.3, 13.9, 12.2. HR-MS (ESI): *m/z* calcd for $C_{19}H_{22}NaO_4$ ($[M + Na]^+$) 337.1410, found 337.1411.

(7-Isovaleryloxy-8-isoprenyl)coumarin (Os6). White crystals; mp 115.1-115.8 °C; 46% yield; ^{1}H NMR (500 MHz, $CDCl_3$): δ 7.83 (d, *J* = 9.4 Hz, 1H), 7.40 (d, *J* = 8.1 Hz, 1H), 6.87 (d, *J* = 7.8 Hz, 1H), 6.28 (d, *J* = 9.2 Hz, 1H), 5.16 (t, *J* = 7.4 Hz, 1H), 3.39 (d, *J* = 7.2 Hz, 2H), 2.47-2.52 (m, 1H), 2.19 (d, *J* = 9.8 Hz, 2H), 1.78 (s, 3H), 1.63 (s, 3H), 1.03 (s, 3H), 0.91 (s, 3H). ^{13}C NMR (125 MHz, $CDCl_3$): δ 168.8, 162.0, 153.4, 151.9, 145.6, 134.8, 124.5, 124.0, 123.4, 118.0, 117.9, 116.9, 42.3, 25.3, 23.6, 21.7, 19.3, 12.4. HR-MS (ESI): *m/z* calcd for $C_{19}H_{22}NaO_4$ ($[M + Na]^+$) 337.1410, found 337.1411.

(7-Hexanoyloxy-8-isoprenyl)coumarin (Os7). White crystals; mp 112.2-113.0 °C; 40% yield; ^{1}H NMR (500 MHz, $CDCl_3$): δ 7.84 (d, *J* = 9.2 Hz, 1H), 7.36 (d, *J* = 8.2 Hz, 1H), 6.82 (d, *J* = 7.8 Hz, 1H), 6.21 (d,

J = 9.2 Hz, 1H), 5.24 (t, *J* = 7.4 Hz, 1H), 3.37 (d, *J* = 7.2 Hz, 2H), 2.23-2.32 (m, 2H), 1.81 (s, 3H), 1.60 (s, 3H), 1.53 (t, *J* = 7.8 Hz, 2H), 1.34 (t, *J* = 7.5 Hz, 2H), 1.27 (t, *J* = 8.9 Hz, 2H), 0.91 (t, *J* = 7.2 Hz, 3H). ^{13}C NMR (125 MHz, $CDCl_3$): δ 169.0, 162.0, 153.4, 151.9, 145.6, 134.8, 124.5, 124.0, 123.4, 118.0, 117.9, 116.9, 33.2, 31.9, 25.3, 24.8, 22.8, 19.3, 14.2, 12.2. HR-MS (ESI): *m/z* calcd for $C_{20}H_{24}NaO_4$ ([M + Na]$^+$) 351.1567, found 351.1568.

(7-Isohexanoyloxy-8-isoprenyl)coumarin (Os8). White crystals; mp 115.4-116.0 °C; 38% yield; ^{1}H NMR (500 MHz, $CDCl_3$): δ 7.85 (d, *J* = 9.2 Hz, 1H), 7.39 (d, *J* = 8.2 Hz, 1H), 6.82 (d, *J* = 7.8 Hz, 1H), 6.23 (d, *J* = 9.2 Hz, 1H), 5.16 (t, *J* = 7.4 Hz, 1H), 3.45 (d, *J* = 7.2 Hz, 2H), 2.16-2.23 (m, 2H), 1.78 (s, 3H), 1.61 (s, 3H), 1.83 (t, *J* = 7.5 Hz, 1H), 1.53 (t, *J* = 10.5 Hz, 2H), 1.03 (s, 3H), 0.87 (s, 3H). ^{13}C NMR (125 MHz, $CDCl_3$): δ 169.0, 162.0, 153.4, 151.9, 145.6, 134.8, 124.5, 124.0, 123.4, 118.0, 117.9, 116.9, 34.5, 30.4, 27.9, 25.1, 22.8, 14.2, 12.4. HR-MS (ESI): *m/z* calcd for $C_{20}H_{24}NaO_4$ ([M + Na]$^+$) 351.1567, found 351.1568.

(7-Benzoyloxy-8-isoprenyl)coumarin (Os9). White crystals; mp 123.4-123.9 °C; 68% yield; ^{1}H NMR (500 MHz, $CDCl_3$): δ 8.25 (d, *J* = 8.3 Hz, 5H), 7.82 (d, *J* = 9.2 Hz, 1H), 7.49 (d, *J* = 8.2 Hz, 1H), 6.97 (d, *J* = 7.8 Hz, 1H), 6.43 (d, *J* = 9.2 Hz, 1H), 5.86 (t, *J* = 7.4 Hz, 1H), 3.25 (d, *J* = 7.2 Hz, 2H), 1.78 (s, 3H), 1.62 (s, 3H). ^{13}C NMR (125 MHz, $CDCl_3$): δ 167.0, 164.0, 152.2, 151.7, 144.2, 134.6, 133.4, 130.8, 130.1, 128.6, 124.6, 124.0, 123.7, 118.8, 117.3, 115.2, 25.3, 19.2, 12.5. HR-MS (ESI): *m/z* calcd for $C_{21}H_{18}NaO_4$ ([M + Na]$^+$) 357.1098, found 357.1099.

7-(2-Fluorobenzoyloxy)-8-isoprenyl]coumarin (Os10). White crystals; mp 121.3-122.2 °C; 47% yield; ^{1}H NMR (500 MHz, $CDCl_3$): δ 8.23 (d, *J* = 8.3 Hz, 1H), 7.80 (d, *J* = 9.2 Hz, 1H), 7.59 (d, *J* = 9.2 Hz, 1H), 7.49 (d, *J* = 8.2 Hz, 1H), 7.46 (t, *J* = 9.2 Hz, 1H), 7.27 (t, *J* = 9.2 Hz, 1H), 6.91 (d, *J* = 7.8 Hz, 1H), 6.45 (d, *J* = 9.2 Hz, 1H), 5.86 (t, *J* = 7.4 Hz, 1H), 3.23 (d, *J* = 7.2 Hz, 2H), 1.76 (s, 3H), 1.61 (s, 3H). ^{13}C NMR (125 MHz, $CDCl_3$): δ 164.0, 163.6, 162.5, 153.4, 151.9, 145.6, 135.3, 134.7, 131.4, 130.6, 124.8, 124.4, 123.4, 118.6, 117.9, 117.5, 116.9, 115.0, 25.1, 19.3, 12.4. HR-MS (ESI): *m/z* calcd for $C_{21}H_{17}FNaO_4$ ([M + Na]$^+$) 375.1004, found 375.1004.

[7-(3-Fluorobenzoyloxy)-8-isoprenyl]coumarin (Os11). White crystals; mp 122.5-123.3 °C; 58% yield; ^{1}H NMR (500 MHz, $CDCl_3$): δ 8.03 (d, *J* = 8.3 Hz, 1H), 7.85 (d, *J* = 9.2 Hz, 1H), 7.82 (d, *J* = 9.2 Hz, 1H), 7.52 (d, *J* = 9.2 Hz, 1H), 7.39 (t, *J* = 9.2 Hz, 1H), 7.22 (t, *J* = 9.2 Hz, 1H), 6.97 (d, *J* = 7.8 Hz, 1H), 6.45 (d, *J* = 9.2 Hz, 1H), 5.83 (t, *J* = 7.4 Hz, 1H), 3.17 (d, *J* = 7.2 Hz, 2H), 1.78 (s, 3H), 1.62 (s, 3H). ^{13}C NMR (125 MHz, $CDCl_3$): δ 165.0, 164.0, 162.0, 153.3, 151.9, 145.6, 134.7, 132.2, 131.1, 130.5, 125.7, 124.8, 124.1, 123.2, 120.8, 118.3, 117.9, 117.1, 25.1, 19.3, 12.1. HR-MS (ESI): *m/z* calcd for $C_{21}H_{17}FNaO_4$ ([M + Na]$^+$) 375.1004, found 375.1004.

[7-(4-Fluorobenzoyloxy)-8-isoprenyl]coumarin (Os12). White crystals; mp 121.7-122.5 °C; 42% yield; ^{1}H NMR (500 MHz, $CDCl_3$): δ 8.13 (d, *J* = 8.3 Hz, 2H), 7.82 (d, *J* = 9.2 Hz, 1H), 7.53 (d, *J* = 9.2 Hz, 1H),

7.12 (d, *J* = 9.2 Hz, 2H), 6.99 (d, *J* = 7.8 Hz, 1H), 6.47 (d, *J* = 9.2 Hz, 1H), 5.86 (t, *J* = 7.4 Hz, 1H), 3.22 (d, *J* = 7.2 Hz, 2H), 1.76 (s, 3H), 1.61 (s, 3H). ^{13}C NMR (125 MHz, $CDCl_3$): δ 167.3, 164.2, 162.6, 153.8, 151.7, 145.6, 134.7, 131.7, 130.5, 126.2, 124.5, 124.0, 123.6, 120.8, 118.0, 117.7, 25.3, 19.6, 12.3. HR-MS (ESI): *m/z* calcd for $C_{21}H_{17}FNaO_4$ ($[M + Na]^+$) 375.1004, found 375.1004.

[7-(2-Chlorobenzoyloxy)-8-isoprenyl]coumarin (Os13). White crystals; mp 119.6-120.3 °C; 52% yield; ^{1}H NMR (500 MHz, $CDCl_3$): δ 8.13 (d, *J* = 8.3 Hz, 1H), 7.82 (d, *J* = 9.2 Hz, 1H), 7.53 (d, *J* = 9.2 Hz, 1H), 7.45 (d, *J* = 8.2 Hz, 1H), 7.42 (t, *J* = 9.2 Hz, 1H), 7.29 (t, *J* = 9.2 Hz, 1H), 6.95 (d, *J* = 7.8 Hz, 1H), 6.44 (d, *J* = 9.2 Hz, 1H), 5.81 (t, *J* = 7.4 Hz, 1H), 3.22 (d, *J* = 7.2 Hz, 2H), 1.76 (s, 3H), 1.61 (s, 3H). ^{13}C NMR (125 MHz, $CDCl_3$): δ 164.0, 162.0, 153.3, 151.7, 145.6, 135.6, 135.1, 134.7, 131.4, 130.6, 128.8, 126.5, 124.5, 124.0, 123.4, 118.6, 117.5, 116.8, 25.4, 19.6, 12.4. HR-MS (ESI): *m/z* calcd for $C_{21}H_{17}ClNaO_4$ ($[M + Na]^+$) 391.0708, found 391.0709.

[7-(3-Chlorobenzoyloxy)-8-isoprenyl]coumarin (Os14). White crystals; mp 117.3-117.9 °C; 54% yield; ^{1}H NMR (500 MHz, $CDCl_3$): δ 8.17 (d, *J* = 8.3 Hz, 1H), 8.02 (d, *J* = 8.3 Hz, 1H), 7.83 (d, *J* = 9.2 Hz, 1H), 7.53 (d, *J* = 7.8 Hz, 1H), 7.51 (d, *J* = 7.2 Hz, 1H), 7.37 (t, *J* = 7.9 Hz, 1H), 6.96 (d, *J* = 7.8 Hz, 1H), 6.42 (d, *J* = 9.2 Hz, 1H), 5.84 (t, *J* = 7.4 Hz, 1H), 3.22 (d, *J* = 7.2 Hz, 2H), 1.76 (s, 3H), 1.61 (s, 3H). ^{13}C NMR (125 MHz, $CDCl_3$): δ 163.0, 161.0, 153.7, 151.2, 144.5, 134.7, 134.1, 133.4, 132.0, 130.5, 129.7, 128.1, 124.5, 124.0, 123.4, 118.1, 117.5, 116.9, 25.3, 19.2, 12.4. HR-MS (ESI): *m/z* calcd for $C_{21}H_{17}ClNaO_4$ ($[M + Na]^+$) 391.0708, found 391.0709.

[7-(4-Chlorobenzoyloxy)-8-isoprenyl]coumarin (Os15). White crystals; mp 117.8-118.5 °C; 38% yield; ^{1}H NMR (500 MHz, $CDCl_3$) δ 8.08 (d, *J* = 8.3 Hz, 2H), 7.86 (d, *J* = 7.2 Hz, 1H), 7.53 (d, *J* = 9.2 Hz, 1H), 7.42 (d, *J* = 9.2 Hz, 2H), 6.94 (d, *J* = 7.8 Hz, 1H), 6.45 (d, *J* = 9.2 Hz, 1H), 5.82 (t, *J* = 7.4 Hz, 1H), 3.25 (d, *J* = 7.2 Hz, 2H), 1.78 (s, 3H), 1.62 (s, 3H). ^{13}C NMR (125 MHz, $CDCl_3$): δ 164.0, 162.0, 153.4, 151.9, 145.2, 139.0, 134.7, 131.5, 128.8, 128.5, 124.5, 124.0, 123.4, 120.8, 118.0, 117.9, 25.3, 19.3, 12.4. HR-MS (ESI): *m/z* calcd for $C_{21}H_{17}ClNaO_4$ ($[M + Na]^+$) 391.0708, found 391.0709.

[7-(2-Bromobenzoyloxy)-8-isoprenyl]coumarin (Os16). White crystals; mp 112.3-112.8 °C; 44% yield; ^{1}H NMR (500 MHz, $CDCl_3$): δ 8.03 (d, *J* = 8.3 Hz, 1H), 7.83 (d, *J* = 9.2 Hz, 1H), 7.58 (d, *J* = 9.2 Hz, 1H), 7.51 (d, *J* = 7.2 Hz, 1H), 7.40 (d, *J* = 8.2 Hz, 1H), 7.35 (t, *J* = 9.2 Hz, 1H), 6.92 (d, *J* = 7.8 Hz, 1H), 6.41 (d, *J* = 9.2 Hz, 1H), 5.83 (t, *J* = 7.4 Hz, 1H), 3.22 (d, *J* = 7.2 Hz, 2H), 1.77 (s, 3H), 1.63 (s, 3H). ^{13}C NMR (125 MHz, $CDCl_3$): δ 164.0, 162.0, 153.6, 151.9, 145.4, 135.9, 134.7, 133.9, 132.3, 131.7, 127.4, 124.7, 124.5, 124.0, 123.1, 118.6, 117.2, 116.8, 25.3, 19.3, 12.2. HR-MS (ESI): *m/z* calcd for $C_{21}H_{17}BrNaO_4$ ($[M + Na]^+$) 435.0203, found 435.0204.

[7-(3-Bromobenzoyloxy)-8-isoprenyl]coumarin (Os17). White crystals; mp 115.6-116.2 °C; 45% yield; ^{1}H NMR (500 MHz, $CDCl_3$): δ 8.34 (d, *J* = 8.3 Hz, 1H), 8.09 (d, *J* = 8.3 Hz, 1H), 7.86 (d, *J* = 9.2 Hz, 1H), 7.68 (d, *J* = 7.8 Hz, 1H), 7.53 (d, *J* = 7.2 Hz, 1H), 7.32 (t, *J* = 7.9 Hz, 1H), 6.99 (d, *J* = 7.8 Hz, 1H), 6.45

(d, *J* = 9.2 Hz, 1H), 5.83 (t, *J* = 7.4 Hz, 1H), 3.26 (d, *J* = 7.2 Hz, 2H), 1.76 (s, 3H), 1.62 (s, 3H). ^{13}C NMR (125 MHz, $CDCl_3$): δ 164.0, 162.0, 153.4, 151.9, 145.6, 137.0, 134.4, 133.2, 132.8, 130.6, 124.7, 124.1, 123.7, 123.2, 118.3, 117.9, 116.9, 25.6, 19.3, 12.2. HR-MS (ESI): *m/z* calcd for $C_{21}H_{17}BrNaO_4$ ([M + Na]$^+$) 435.0203, found 435.0204.

[7-(4-Bromobenzoyloxy)-8-isoprenyl]coumarin (Os18). White crystals; mp 112.6-113.3 °C; 52% yield; ^{1}H NMR (500 MHz, $CDCl_3$): δ 8.03 (d, *J* = 8.3 Hz, 2H), 7.83 (d, *J* = 7.2 Hz, 1H), 7.58 (d, *J* = 9.2 Hz, 2H), 7.51 (d, *J* = 9.2 Hz, 1H), 6.96 (d, *J* = 7.8 Hz, 1H), 6.42 (d, *J* = 9.2 Hz, 1H), 5.88 (t, *J* = 7.4 Hz, 1H), 3.26 (d, *J* = 7.2 Hz, 2H), 1.76 (s, 3H), 1.62 (s, 3H). ^{13}C NMR (125 MHz, $CDCl_3$): δ 164.0, 162.0, 153.7, 151.4, 145.6, 134.7, 132.3, 131.7, 129.6, 128.3, 124.5, 124.1, 123.4, 118.0, 117.9, 116.9, 25.1, 19.4, 12.4. HR-MS (ESI): *m/z* calcd for $C_{21}H_{17}BrNaO_4$ ([M + Na]$^+$) 435.0203, found 435.0204.

[7-(2-Cyanobenzoyloxy)-8-isoprenyl]coumarin (Os19). Yellow oil; 43% yield; ^{1}H NMR (500 MHz, $CDCl_3$): δ 8.32 (d, *J* = 8.3 Hz, 1H), 7.82 (d, *J* = 9.2 Hz, 1H), 7.69 (d, *J* = 7.8 Hz, 1H), 7.64 (d, *J* = 8.3 Hz, 1H), 7.63 (d, *J* = 7.2 Hz, 1H), 7.51 (t, *J* = 7.9 Hz, 1H), 6.93 (d, *J* = 7.8 Hz, 1H), 6.43 (d, *J* = 9.2 Hz, 1H), 5.85 (t, *J* = 7.4 Hz, 1H), 3.27 (d, *J* = 7.2 Hz, 2H), 1.78 (s, 3H), 1.61 (s, 3H). ^{13}C NMR (125 MHz, $CDCl_3$): δ 163.0, 161.0, 153.8, 151.1, 145.8, 134.9, 134.4, 134.1, 132.7, 131.6, 130.8, 124.7, 124.1, 123.3, 118.5, 117.6, 116.5, 116.3, 114.1, 25.6, 19.3, 12.2. HR-MS (ESI): *m/z* calcd for $C_{22}H_{18}NO_4$ ([M + H]$^+$) 360.1231, found 360.1231.

[7-(3-Cyanobenzoyloxy)-8-isoprenyl]coumarin (Os20). Yellow oil; 53% yield; ^{1}H NMR (500 MHz, $CDCl_3$): δ 8.44 (d, *J* = 8.3 Hz, 1H), 8.39 (d, *J* = 8.3 Hz, 1H), 7.86 (d, *J* = 9.2 Hz, 1H), 7.76 (d, *J* = 7.8 Hz, 1H), 7.59 (d, *J* = 7.2 Hz, 1H), 7.51 (t, *J* = 7.9 Hz, 1H), 6.96 (d, *J* = 7.8 Hz, 1H), 6.45 (d, *J* = 9.2 Hz, 1H), 5.81 (t, *J* = 7.4 Hz, 1H), 3.28 (d, *J* = 7.2 Hz, 2H), 1.79 (s, 3H), 1.63 (s, 3H). ^{13}C NMR (125 MHz, $CDCl_3$): δ 164.0, 162.0, 153.8, 151.3, 145.7, 137.4, 134.7, 134.4, 133.6, 131.3, 129.1, 124.5, 124.0, 123.4, 118.6, 117.5, 116.5, 112.4, 25.4, 19.1, 12.2. HR-MS (ESI): *m/z* calcd for $C_{22}H_{18}NO_4$ ([M + H]$^+$) 360.1231, found 360.1231.

[7-(4-Cyanobenzoyloxy)-8-isoprenyl]coumarin (Os21). Yellow oil; 57% yield; ^{1}H NMR (500 MHz, $CDCl_3$): δ 8.34 (d, *J* = 8.3 Hz, 2H), 7.68 (d, *J* = 9.2 Hz, 2H), 7.84 (d, *J* = 7.2 Hz, 1H), 7.53 (d, *J* = 9.2 Hz, 1H), 6.99 (d, *J* = 7.8 Hz, 1H), 6.44 (d, *J* = 9.2 Hz, 1H), 5.83 (t, *J* = 7.4 Hz, 1H), 3.24 (d, *J* = 7.2 Hz, 2H), 1.76 (s, 3H), 1.62 (s, 3H). ^{13}C NMR (125 MHz, $CDCl_3$): δ 164.0, 162.0, 153.4, 151.9, 145.8, 134.7, 131.9, 130.8, 124.5, 124.0, 123.6, 118.3, 117.9, 117.7, 116.9, 116.5, 25.4, 19.3, 12.4. HR-MS (ESI): *m/z* calcd for $C_{22}H_{18}NO_4$ ([M + H]$^+$) 360.1231, found 360.1231.

[7-(2-Methylbenzoyloxy)-8-isoprenyl]coumarin (Os22). White crystals; mp 123.4-124.2 °C; 62% yield; ^{1}H NMR (500 MHz, $CDCl_3$): δ 8.08 (d, *J* = 8.3 Hz, 1H), 7.82 (d, *J* = 7.8 Hz, 1H), 7.51 (t, *J* = 7.9 Hz, 1H), 7.41 (d, *J* = 8.3 Hz, 1H), 7.27 (d, *J* = 7.2 Hz, 1H), 7.21 (d, *J* = 9.2 Hz, 1H), 6.93 (d, *J* = 7.8 Hz, 1H), 6.47 (d, *J* = 9.2 Hz, 1H), 5.83 (t, *J* = 7.4 Hz, 1H), 3.24 (d, *J* = 7.2 Hz, 2H), 2.32 (s, 3H), 1.72 (s, 3H), 1.61 (s,

3H). ^{13}C NMR (125 MHz, $CDCl_3$): δ 164.0, 162.0, 153.7, 151.8, 145.2, 139.3, 134.7, 133.6, 131.3, 130.0, 129.3, 125.4, 124.5, 124.0, 123.1, 118.3, 117.7, 116.4, 25.3, 19.2, 14.1, 12.4. HR-MS (ESI): *m/z* calcd for $C_{22}H_{20}NaO_4$ ($[M + Na]^+$) 371.1255, found 371.1256.

[7-(3-Methylbenzoyloxy)-8-isoprenyl]coumarin (Os23). White crystals; mp 125.2-125.8 °C; 46% yield; ^{1}H NMR (500 MHz, $CDCl_3$): δ 8.02 (d, *J* = 8.3 Hz, 1H), 7.94 (d, *J* = 9.2 Hz, 1H), 7.89 (d, *J* = 7.8 Hz, 1H), 7.53 (t, *J* = 7.9 Hz, 1H), 7.31 (d, *J* = 8.3 Hz, 1H), 7.29 (d, *J* = 7.2 Hz, 1H), 6.93 (d, *J* = 7.8 Hz, 1H), 6.47 (d, *J* = 9.2 Hz, 1H), 5.85 (t, *J* = 7.4 Hz, 1H), 3.26 (d, *J* = 7.2 Hz, 2H), 2.37 (s, 3H), 1.74 (s, 3H), 1.62 (s, 3H). ^{13}C NMR (125 MHz, $CDCl_3$): δ 164.0, 162.0, 153.5, 151.6, 145.7, 137.6, 134.7, 134.4, 130.9, 130.4, 128.3, 127.1, 124.5, 124.1, 123.4, 118.6, 117.9, 116.8, 25.6, 20.9, 19.3, 12.4. HR-MS (ESI): *m/z* calcd for $C_{22}H_{20}NaO_4$ ($[M + Na]^+$) 371.1255, found 371.1256.

[7-(4-Methylbenzoyloxy)-8-isoprenyl]coumarin (Os24). White crystals; mp 121.6-122.4 °C; 41% yield; ^{1}H NMR (500 MHz, $CDCl_3$): δ 8.04 (d, *J* = 8.3 Hz, 2H), 7.82 (d, *J* = 7.2 Hz, 1H), 7.53 (d, *J* = 9.2 Hz, 1H), 7.22 (d, *J* = 9.2 Hz, 2H), 6.94 (d, *J* = 7.8 Hz, 1H), 6.41 (d, *J* = 9.2 Hz, 1H), 5.85 (t, *J* = 7.4 Hz, 1H), 3.24 (d, *J* = 7.2 Hz, 2H), 2.35 (s, 3H), 1.78 (s, 3H), 1.62 (s, 3H). ^{13}C NMR (125 MHz, $CDCl_3$): δ 164.0, 162.0, 153.7, 151.6, 145.7, 142.9, 134.4, 130.8, 129.1, 127.6, 124.5, 124.1, 123.4, 118.3, 117.6, 116.9, 25.3, 20.9, 19.6, 12.4. HR-MS (ESI): *m/z* calcd for $C_{22}H_{20}NaO_4$ ($[M + Na]^+$) 371.1255, found 371.1256.

[7-(2-Methoxybenzoyloxy)-8-isoprenyl]coumarin (Os25). White crystals; mp 128.2-128.7 °C; 48% yield; ^{1}H NMR (500 MHz, $CDCl_3$): δ 8.04 (d, *J* = 8.3 Hz, 1H), 7.87 (d, *J* = 7.8 Hz, 1H), 7.53 (t, *J* = 7.9 Hz, 1H), 7.43 (d, *J* = 8.3 Hz, 1H), 6.99 (d, *J* = 7.8 Hz, 1H), 6.97 (d, *J* = 7.2 Hz, 1H), 6.92 (d, *J* = 9.2 Hz, 1H), 6.44 (d, *J* = 9.2 Hz, 1H), 5.81 (t, *J* = 7.4 Hz, 1H), 3.74 (s, 3H), 3.21 (d, *J* = 7.2 Hz, 2H), 1.73 (s, 3H), 1.62 (s, 3H). ^{13}C NMR (125 MHz, $CDCl_3$): δ 164.0, 163.6, 162.0, 153.6, 151.9, 145.6, 134.9, 134.7, 131.1, 124.5, 124.0, 123.7, 120.7, 118.6, 117.6, 116.9, 116.3, 114.0, 56.3, 25.2, 19.3, 12.4. HR-MS (ESI): *m/z* calcd for $C_{22}H_{20}NaO_5$ ($[M + Na]^+$) 387.1204, found 387.1204.

[7-(3-Methoxybenzoyloxy)-8-isoprenyl]coumarin (Os26). White crystals; mp 126.5-127.3 °C; 38% yield; ^{1}H NMR (500 MHz, $CDCl_3$): δ 7.83 (d, *J* = 7.8 Hz, 1H), 7.72 (d, *J* = 8.3 Hz, 1H), 7.64 (d, *J* = 9.2 Hz, 1H), 7.53 (t, *J* = 7.9 Hz, 1H), 7.32 (d, *J* = 8.3 Hz, 1H), 7.09 (d, *J* = 7.2 Hz, 1H), 6.97 (d, *J* = 7.8 Hz, 1H), 6.45 (d, *J* = 9.2 Hz, 1H), 5.88 (t, *J* = 7.4 Hz, 1H), 3.73 (s, 3H), 3.23 (d, *J* = 7.2 Hz, 2H), 1.74 (s, 3H), 1.62 (s, 3H). ^{13}C NMR (125 MHz, $CDCl_3$): δ 164.0, 162.0, 161.9, 153.4, 151.9, 145.6, 134.7, 131.6, 129.3, 124.3, 124.4, 123.4, 122.4, 119.5, 118.9, 117.9, 116.8, 115.4, 56.9, 25.4, 19.3, 12.4. HR-MS (ESI): *m/z* calcd for $C_{22}H_{20}NaO_5$ ($[M + Na]^+$) 387.1204, found 387.1204.

[7-(4-Methoxybenzoyloxy)-8-isoprenyl]coumarin (Os27). White crystals; mp 125.3-125.8 °C; 41% yield; ^{1}H NMR (500 MHz, $CDCl_3$): δ 8.07 (d, *J* = 8.3 Hz, 2H), 7.82 (d, *J* = 7.2 Hz, 1H), 7.51 (d, *J* = 9.2 Hz, 1H), 6.96 (d, *J* = 7.8 Hz, 1H), 6.92 (d, *J* = 9.2 Hz, 2H), 6.45 (d, *J* = 9.2 Hz, 1H), 5.85 (t, *J* = 7.4 Hz, 1H), 3.75 (s, 3H), 3.22 (d, *J* = 7.2 Hz, 2H), 1.78 (s, 3H), 1.62 (s, 3H). ^{13}C NMR (125 MHz, $CDCl_3$): δ

167.3, 164.0, 162.0, 153.6, 151.8, 145.3, 134.9, 131.1, 124.3, 124.0, 123.7, 122.9, 118.4, 117.9, 114.0, 56.7, 25.3, 19.5, 12.1. HR-MS (ESI): *m/z* calcd for $C_{22}H_{20}NaO_5$ ($[M + Na]^+$) 387.1204, found 387.1204.

[7-(2-Hydroxybenzoyloxy)-8-isoprenyl]coumarin (Os28). Yellow oil; 56% yield; ^{1}H NMR (500 MHz, $CDCl_3$): δ 7.98 (d, *J* = 8.3 Hz, 1H), 7.82 (d, *J* = 7.8 Hz, 1H), 7.51 (t, *J* = 7.9 Hz, 1H), 7.34 (d, *J* = 8.3 Hz, 1H), 6.99 (d, *J* = 7.8 Hz, 1H), 6.96 (d, *J* = 7.2 Hz, 1H), 6.88 (d, *J* = 9.2 Hz, 1H), 6.45 (d, *J* = 9.2 Hz, 1H), 5.83 (t, *J* = 7.4 Hz, 1H), 3.23 (d, *J* = 7.2 Hz, 2H), 1.76 (s, 3H), 1.62 (s, 3H). ^{13}C NMR (125 MHz, $CDCl_3$): δ 164.0, 162.0, 158.9, 153.4, 151.7, 145.2, 135.1, 134.6, 131.5, 124.5, 124.0, 123.4, 121.0, 118.2, 117.8, 117.4, 116.9, 115.6, 25.4, 19.6, 12.4. HR-MS (ESI): *m/z* calcd for $C_{21}H_{19}O_5$ ($[M + H]^+$) 351.1227, found 351.1228.

[7-(3-Hydroxybenzoyloxy)-8-isoprenyl]coumarin (Os29). Yellow oil; 52% yield; ^{1}H NMR (500 MHz, $CDCl_3$): δ 7.86 (d, *J* = 7.8 Hz, 1H), 7.70 (d, *J* = 8.3 Hz, 1H), 7.61 (d, *J* = 9.2 Hz, 1H), 7.51 (t, *J* = 7.9 Hz, 1H), 7.24 (d, *J* = 8.3 Hz, 1H), 6.98 (d, *J* = 7.2 Hz, 1H), 6.92 (d, *J* = 7.8 Hz, 1H), 6.43 (d, *J* = 9.2 Hz, 1H), 5.83 (t, *J* = 7.4 Hz, 1H), 3.21 (d, *J* = 7.2 Hz, 2H), 1.73 (s, 3H), 1.62 (s, 3H). ^{13}C NMR (125 MHz, $CDCl_3$): δ 163.0, 161.0, 157.2, 153.7, 151.6, 145.3, 134.5, 132.0, 129.8, 124.5, 124.0, 123.3, 122.7, 120.9, 118.6, 117.9, 117.3, 116.7, 25.3, 19.2, 12.4. HR-MS (ESI): *m/z* calcd for $C_{21}H_{19}O_5$ ($[M + H]^+$) 351.1227, found 351.1228.

[7-(4-Hydroxybenzoyloxy)-8-isoprenyl]coumarin (Os30). Yellow oil; 58% yield; ^{1}H NMR (500 MHz, $CDCl_3$): δ 7.97 (d, *J* = 8.3 Hz, 2H), 7.81 (d, *J* = 7.2 Hz, 1H), 7.53 (d, *J* = 9.2 Hz, 1H), 6.99 (d, *J* = 7.8 Hz, 1H), 6.88 (d, *J* = 9.2 Hz, 2H), 6.43 (d, *J* = 9.2 Hz, 1H), 5.85 (t, *J* = 7.4 Hz, 1H), 3.24 (d, *J* = 7.2 Hz, 2H), 1.73 (s, 3H), 1.62 (s, 3H). ^{13}C NMR (125 MHz, $CDCl_3$): δ 164.3, 162.7, 162.0, 153.4, 151.9, 145.6, 134.7, 131.5, 124.5, 124.0, 123.5, 123.0, 118.3, 117.6, 116.9, 115.6, 25.1, 19.3, 12.4. HR-MS (ESI): *m/z* calcd for $C_{21}H_{19}O_5$ ($[M + H]^+$) 351.1227, found 351.1228.

[7-(2, 4-Dichlorobenzoyloxy)-8-isoprenyl]coumarin (Os31). White crystals; mp 108.4-109.2 °C; 47% yield; ^{1}H NMR (500 MHz, $CDCl_3$): δ 8.06 (d, *J* = 7.8 Hz, 1H), 7.80 (d, *J* = 8.3 Hz, 1H), 7.53 (t, *J* = 7.9 Hz, 1H), 7.41 (d, *J* = 9.2 Hz, 1H), 7.30 (d, *J* = 8.3 Hz, 1H), 6.97 (d, *J* = 7.2 Hz, 1H), 6.44 (d, *J* = 9.2 Hz, 1H), 5.84 (t, *J* = 7.4 Hz, 1H), 3.23 (d, *J* = 7.2 Hz, 2H), 1.76 (s, 3H), 1.63 (s, 3H). ^{13}C NMR (125 MHz, $CDCl_3$): δ 164.0, 162.0, 153.4, 151.9, 145.6, 140.4, 136.8, 134.7, 132.9, 129.7, 129.1, 126.9, 124.6, 124.0, 123.2, 118.8, 117.9, 116.9, 25.1, 19.3, 12.4. HR-MS (ESI): *m/z* calcd for $C_{21}H_{17}Cl_2O_4$ ($[M + H]^+$) 403.0499, found 403.0499.

[7-(3, 5-Difluorobenzoyloxy)-8-isoprenyl]coumarin (Os32). White crystals; mp 105.7-106.5 °C; 54% yield; ^{1}H NMR (500 MHz, $CDCl_3$): δ 7.82 (d, *J* = 8.3 Hz, 1H), 7.62 (d, *J* = 9.2 Hz, 2H), 7.51 (t, *J* = 7.9 Hz, 1H), 6.97 (d, *J* = 7.2 Hz, 1H), 6.93 (d, *J* = 8.3 Hz, 1H), 6.43 (d, *J* = 9.2 Hz, 1H), 5.82 (t, *J* = 7.4 Hz, 1H), 3.23 (d, *J* = 7.2 Hz, 2H), 1.72 (s, 3H), 1.62 (s, 3H). ^{13}C NMR (125 MHz, $CDCl_3$): δ 164.0, 163.6, 162.0, 153.1, 151.9, 145.6, 134.7, 133.8, 124.5, 124.0, 123.4, 118.6, 117.9, 116.5, 112.7, 107.7, 25.3, 19.3,

12.4. HR-MS (ESI): *m/z* calcd for $C_{21}H_{17}F_2O_4$ ($[M + H]^+$) 371.1090, found 371.1090.

Biological Assays. The pathogenic fungi *Botrytis cinerea*, *Valsa mali* Miyabe et Yamada, *Alternaria brassicicola* (Schweinitz) Wilts., *Fusahum graminearum* Sehw., *Rhizoctonia solani*, *Colletotrichum gloeosporioides* Penz. and *Sclerotinia sclerotiorum* were provided by the Center of Pesticide Research, Northwest A&F University, China. These fungi were grown on potato dextrose agar (PDA) plates at 25 °C and maintained at 4 °C with periodic subculturing.

***In Vitro* Antifungal Assay.** According to the mycelium linear growth rate method reported previously,[38] the antifungal activities *in vitro* of compounds against seven strains of plant pathogenic fungi were tested. The compounds with higher initial activities against *F. graminearum* Sehw. and *R. solani* were selected to assay 50% inhibition concentration values (IC_{50}). In order to get a series of stock solutions, the test compound (2 mM) was diluted with 5% DMSO aqueous solution by double-fold dilution method. Each stock solution (10 mL) was mixed with the autoclaved PDA medium (190 mL) to provide a set of mediums with different concentrations of the test compound (3.125, 6.25, 12.5, 25, 50 and 100 μM). The culture medium containing only 0.25% DMSO was used as a blank control, and carbendazim osthole used as positive control. Each test was performed in triplicate. Antifungal toxicity regression equations and IC_{50} values were established according to the method previously reported.[39]

***In Vivo* Antifungal Assay.** Fungi strains and fungicides: The fungal pathogens *B. cinerea* was provided by the Agricultural Culture Collection of China (Yangling, Shaanxi, China). *B. cinerea* was cultured for 2 weeks at 25 °C on potato dextrose agar (PDA) after being retrieved from the storage tube. The stock solution of test compound was diluted with water containing 0.1% tween-80 to 200 μg/mL.

Against the *B. cinerea*: Protective activity of test samples against *B. cinerea* on tomato fruits was determined on following ways. Tomato fruits were surface disinfected in sodium hypochlorite (7%, w/v) solution for 5 min and washed thoroughly with sterile water, then spray tested samples on the tomato fruits until liquid flowed on surface at 24 h before inoculation. Inoculated fruits were placed in plastic boxes at 25 °C with a 16 h photoperiod and 80% relative humidity for disease development, carbendazim was used as the positive control. After 3 days, the average lesion diameter was determined by measuring each lesion in two perpendicular directions. The lengths of the long and short axes were averaged and disease control efficacy was calculated as follows: disease control efficacy = (lesion diameter in the water control-lesion diameter in the treatment)/lesion diameter in the water control * 100.

Against the *B. graminis*: Wheat Seeds were surface disinfected in sodium hypochlorite (7%, w/v) solution for 5 min, washed thoroughly with sterile water, and then germinated in a 9 cm pots. After 14 days, plants were reached the desired leaf stage, the tested samples uniform spray on the leaves 24 h before shaking spores. After inoculation, plants were incubated at 20 °C/15 °C in a growth chamber with cycles of 16 h light and 8 h darkness. Two controls were included in each experiment: untreated leaves and leaves treated with 15% triadimefon. Assessment of disease was made 7 days after inoculation by counting the number of colonies on 2.5 cm of the middle part of the treated leaf area. In most cases, leaves with colonies were assessed visually and classified according to a scale from 0 to 4. In which 0 = leaves with no symptoms, 1 = lesions on＜25%, 2 = lesions on 25-50%, 3 = lesions on 50-75%, and 4 = lesions on 75-100%. The disease index and biocontrol effect meet the following equation.

$$\text{Disease index (\%)} = \frac{\sum(\text{grade of disease severity} \times \text{diseased plants of this grade})}{\text{total plants were assessed} \times \text{the highest grade of disease severity}} \times 100$$

$$\text{Biocontrol effect (\%)} = \frac{\text{disease index of pathogen control} - \text{disease index of bacteria treatment}}{\text{disease index of pathogen control}} \times 100$$

Building and Validation of the QSAR Model. The building and validation of the QSAR model was carried with the common procedure. Briefly, by using of the Gaussian 03W package of programs (Gaussian Inc.), the optimal conformers of the title compounds with the lowest energy were computed at the DFT/6-31G (d) level.[37] Meanwhile, the most stable configurations of the compounds were generated and the corresponding ".log" and ".chk" files were gained. Afterwards, the calculated results were transformed into a form compatible with CODESSA 2.7.15 using Ampac 9.1.3.[41,42] At last, all of the molecular descriptors involved in these compounds were calculated by CODESSA 2.7.15, and the heuristic method analysis was used to build the QSAR model, which determinate the most significant structural features for antifungal activity against *R. solani*. During the model development process, the squared correction coefficient (R^2), the squared standard error of the estimates (S^2), and the Fisher significance ratio (F) were used to clarify the standards of statics. Moreover, the tested IC_{50} values were converted into the corresponding plog IC_{50} values and used as dependent variables to get better linear regression. The quality of the final model was ensured by using internal validation and the "leave-one-out" cross-validation methods.[43]

ACKNOWLEDGEMENTS

We greatly appreciate the funding support for this research provided by the Natural Science Foundation of Shaanxi Province (No. 2021JQ-842) and Shengyong Zhang Academician Project of Shangluo University

(No. 18 YSZX005). We also thank Northwest A&F University for the ^{1}H NMR, ^{13}C NMR, and HR-ESI-MS spectral data.

REFERENCES

1. G. S. Gilbert, *Annu. Rev. Phytopathol.*, 2002, **40**, 13.
2. M. C. Fisher, D. A. Henk, C. J. Briggs, J. S. Brownstein, L. C. Madoff, S. L. McCraw, and S. J. Gurr, *Nature*, 2012, **484**, 186.
3. P. K. Anderson, A. A. Cunningham, N. G. Patel, F. J. Morales, P. R. Epstein, and P. Daszak, *Trends Ecol. Evol.*, 2004, **19**, 535.
4. M. Nucci and K. A. Marr, *Clin. Infect. Dis.*, 2005, **41**, 521.
5. A. Drenth and D. I. Guest, *Annu. Rev. Phytopathol.*, 2016, **54**, 373.
6. T. C. Sparks and B. A. Lorsbach, *Pest Manag. Sci.*, 2017, **73**, 672.
7. T. Hirooka and H. Ishii, *J. Gen. Plant Pathol.*, 2013, **79**, 390.
8. P. E. Russell, *Plant Pathol.*, 2006, **55**, 585.
9. E. D. Franck, L. C. Charles, and O. D. Stephen, *Bioorg. Med. Chem.*, 2009, **17**, 4022.
10. N. Carl, H. Stefan, and R. Lars, *Chem. Commun.*, 2011, **47**, 4062.
11. G. C. Leonard and P. S. Bhupinder, *Pest Manag. Sci.*, 2000, **56**, 649.
12. G. M. Cragg and D. J. Newman, *Biochim. Biophys. Acta*, 2013, **1830**, 3670.
13. L. G. Copping and S. O. Duke, *Pest Manag. Sci.*, 2007, **63**, 524.
14. J. N. Seiber, J. Coats, S. O. Duke, and A. D. Gross, *J. Agric. Food Chem.*, 2014, **62**, 11613.
15. C. L. Cantrell, F. E. Dayan, and S. O. Duke, *J. Nat. Prod.*, 2012, **75**, 1231.
16. T. C. Sparks, D. R. Hahn, and N. V. Garizi, *Pest Manag. Sci.*, 2017, **73**, 700.
17. Y. L. Wu, Y. Q. Gao, D. L. Wang, C. Q. Zhong, J. T. Feng, and X. Zhang, *RSC Adv.*, 2017, **7**, 56496.
18. Q. Zhang, L. Qin, W. He, L. V. Puyvelde, D. Maes, A. Adams, H. Zheng, and N. D. Kimpe, *Planta Med.*, 2007, **73**, 13.
19. J. Agata, G. Aneta, S. W. Krystyna, and S. Andrzej, *Postępy Hig. Med. Dośw.*, 2017, **71**, 411.
20. X. M. Xu, Y. Zhang, D. Qu, T. Jiang, and S. Li, *J. Exp. Clin. Cancer Res.*, 2011, **30**, 33.
21. X. M. Xu, Y. Zhang, D. Qu, H, B. Liu, X. Gu, G. Y. Jiao, and L. Zhao, *Exp. Ther. Med.*, 2013, **5**, 707.
22. J. X. Liu, W. P. Zhang, L. Zhou. X. R. Wang, and Q. S. Lian, *J. Chin. Med. Mater.*, 2005, **28**, 1002.
23. D. P. Yang, H. X. Wang, and Y. Y. Peng, *J. Nanjing Normal Univ.*, 2010, **33**, 76.
24. J. J. Luszczki, E. Wojda, M. Andres-Mach, W. Cisowski, M. Glensk, K. Glowniak, and S. J. Czuczwar, *Epilepsy Res.*, 2009, **85**, 293.
25. S. S. Chu, J. Cao, Q. Z. Liu, S. S. Du, Z. W. Deng, and Z. L. Liu, *Chemija*, 2012, **23**, 108.

26. M. Z. Zhang, R. R. Zhang, J. Q. Wang, X. Yu, Y. L. Zhang, Q. Q. Wang, and W. H. Zhang, *Eur. J. Med. Chem.*, 2016, **124**, 10.
27. A. Andreani, S. Burnelli, M. Granaiola, A. Leoni, A. Locatelli, R. Morigi, M. Rambaldi, L. Varoli, N. Calonghi, C. Cappadone, M. Voltattorni, M. Zini, C. Stefanelli, L. Masotti, and R. H. Shoemaker, *J. Med. Chem.*, 2008, **51**, 7508.
28. D. Sharma, B. Narasimhan, P. Kumar, and A. Jalbout, *Eur. J. Med. Chem.*, 2009, **44**, 1119.
29. P. Sharma, A. Kumar, S. Upadhyay, V. Sahu, and J. Singh, *Eur. J. Med. Chem.*, 2009, **44**, 251.
30. Z. Wang, J. Song, J. Chen, Z. Song, S. Shang, Z. Jiang, and Z. Han, *Bioorg. Med. Chem. Lett.*, 2008, **18**, 2854.
31. M. Karelson, V. S. Lobanov, and A. R. Katritzky, *Chem. Rev.*, 1996, **96**, 1027.
32. F. De Proft, C. Van Alsenoy, A. Peeters, W. Langenaeker, and P. Geerlings, *J. Comput. Chem.*, 2002, **23**, 1198.
33. C. L. Yao, Z. Xue, M. Lian, X. B. Xu, J. Zhao, G. Zhou, Y. Wu, D. M. Yu, and W. Y. Wong, *J. Organomet. Chem.*, 2015, **784**, 31.
34. L. Y. Zhao and S. S. Feng, *J. Colloid Interface Sci.*, 2004, **274**, 55.
35. R. Kumar, A. Kumar, S. Jain, and D. Kaushik, *Eur. J. Med. Chem.*, 2011, **46**, 3543.
36. M. Witschel, *Bioorg. Med. Chem.*, 2009, **17**, 4221.
37. C. K. Z. Andrade, R. O. Rocha, O. E. Vercillo, W. A. Silva, and R. A. F. Matos, *Synlett*, 2003, 2351.
38. L. Fang, M. Wang, S. Gou, X. Liu, H. Zhang, and F. Cao, *J. Med. Chem.*, 2014, **57**, 1116.
39. J. Feng, D. Wang, Y. Wu, H. Yan, and X. Zhang, *Bioorg. Med. Chem. Lett.*, 2013, **23**, 4393.
40. M. J. Frisch, G. W. Trucks, H. B. Schlegel, G. E. Scuseria, M. A. Robb, J. R. Cheeseman, J. A. Montgomery, T. Vreven, K. N. Kudin, and J. C. Burant, Gaussian 03, Gaussian, Inc., Wallingford, CT, USA, 2004.
41. A. Katritsky, M. Karelson, V. S. Lobanov, R. Dennington, T. A. Keith, and R. D. A. T. Keith, Codessa 2.7.15, Semichem, Inc., Shawnee, KS, USA, 2004.
42. M. J. S. Dewar, A. J. Holder, I. Roy, D. Dennington, D. A. Liotard, D. G. Truhlar, T. A. Keith, J. M. Millam, and C. D. Harris, AMPAC 9.3.1, Semichem, Inc., Shawnee, KS, USA, 2004.
43. Y. Gao, X. Tian, J. Li, S. Shang, Z. Song, and M. Shen, *ACS Sustain. Chem. Eng.*, 2016, **4**, 2741.